33RD CONGRESS
OF THE INTERNATIONAL COUNCIL
OF THE AERONAUTICAL SCIENCES
STOCKHOLM, SWEDEN, 4-9 SEPTEMBER, 2022

ICAS 2022 SWEDEN

Influence of Maneuvering Process on Performance Characteristics of Belly Inlet of Aircraft

Xu Binbin, Wu Chaojun, Sun Fuzhen, Tang Jianping, Xiong Wentao

Low Speed Aerodynamics Institute, China Aerodynamics Research and Development Center

Abstract

During the high maneuvering process of aircraft, the aerodynamics characteristics of the inner and outer flow fields of the inlet device are quite different from those when the aircraft maintains a stable attitude angle. The local flow field in inlet presents obvious unsteady properties, which may lead to drastic effect on the aerodynamic performance at the aerodynamics interface plane (AIP) of turbine engine and inlet. Even it may induce engine surge and cause an accident. In order to obtain the influence of maneuvering process on the aerodynamics performance characteristics of aircraft inlet, the dynamic inlet wind tunnel experiment technology was built in ϕ3.2m low speed wind tunnel of the China Aerodynamics Research and Development Center (CARDC). The steady-state inlet experiments and the maneuvering inlet experiments were carried out. The experimental results show that, for the inlet located at the belly of the aircraft, the pitching maneuver has small effect on aerodynamics performance at the AIP of inlet, while the sideslip maneuver has a larger effect on aerodynamics performance at the AIP of inlet. The research results show that there are obvious difference of the aerodynamic characteristics at AIP of the belly inlet between the steady-state conditions and maneuvering process.

Keywords: Belly inlet; Dynamics inlet experiments; pitching maneuver; sideslip maneuver; Total pressure recovery coefficient; Composite distortion factor;

1. Introduction

In the course of fighter maneuvering, the high speed change of aircraft attitude angle leads to obvious unsteady phenomena such as flow parameters at the inlet, total pressure recovery coefficient and total pressure distortion at the outlet. Fast pitching maneuver is a typical maneuver process. During this process, the range of angle of attack of the aircraft can reach more than 90° in a few seconds, and angular speed can reach 30°/s ~ 50°/s. The flow field of the front fuselage has a strong unsteady effect, and the characteristics of internal and external flow field of the inlet are quite different from those of the aircraft in steady and flat flight. The influence of inlet transient distortion characteristics on engine safety is an important part of the evaluation of inlet/engine matching characteristics.

In 1954, the engine surge occurred for SUPER Saber F-100 aircraft, while the maximum angle of attack did not exceed the allowable critical angle in the maneuver flight with large overload. The reason was that the transient distortion of total pressure in the maneuver exceeded the maximum allowable value of the steady-state distortion. In 1966, when an F-111 fighter aircraft was performing high-subsonic maneuvering flight experiment, the engine surge and even the shutdown occurred. The main reason is that the transient distortion value of the inlet during maneuvering was 4% higher than the steady-state distortion value (the maximum allowable steady-state distortion value was 10%, while the actual transient distortion value was 14%). It is not reasonable to measure the safety margin of inlet/engine compatibility only with the maximum distortion under steady-state experimental conditions. It is necessary to conduct detailed research not only on the

steady-state characteristics of the inlet [1] but also the dynamic distortion characteristics under high maneuvering condition through the method of numerical calculation, wind tunnel experiment and flight test [2]. For example, in the 1990s, the wind tunnel experiments and flight experiments were carried out in NASA to study the distortion characteristics of the inlet of F/A-18 fighter during maneuvering [3]-[5], and obtained the distortion characteristics of the inlet under unsteady inlet flow field [6].

Steady-state and maneuvering inlet experiments were carried out in the Φ-3.2m low speed wind tunnel of China Aerodynamics Research and Development Center (CARDC). The influence of maneuvering process on aerodynamic characteristics of aircraft belly inlet was studied. Firstly, the experimental equipment and the experimental technology was introduction. Then, the steady-state and maneuvering inlet experimental of belly inlet are compared, and the experimental results are compared and analyzed.

2. Experiment equipment

2.1 Wind tunnel

The maneuvering inlet experiments were conducted in the Φ-3.2m low speed wind tunnel of CARDC. Φ-3.2m wind tunnel is an open-jet and return flow low speed wind tunnel with a round test section. The diameter and the length of test section are 3.2m and 5m, respectively. The maximum and the minimum steady wind speed in test section are 115m/s and 11.5m/s, respectively.

2.2 Support device

In inlet experiment, the aircraft model is supported by the hollow tail strut. The main body of the model support device is a U-shaped mechanism driven by two hollow torque motors. The tail strut is fixed at the center of a U-shape support mechanism which can be driven to move with a certain angular velocity by two coaxial motors. The maximum angular speed of model is 240 °/s when the mass of model is less than 20kg. The Schematic diagram and the photo are shown in Figure 1 and Figure 2. The air flow driven by ejector flows through the inlet of model and the air support then the u-shaped mechanism and the hollow torque motor, finally reach the ejector. The maximum and minimum angle of attack of support device can reach ±180°. The model attitude angle control precision is 0.05° in steady state and 0.5° in maneuvering condition.

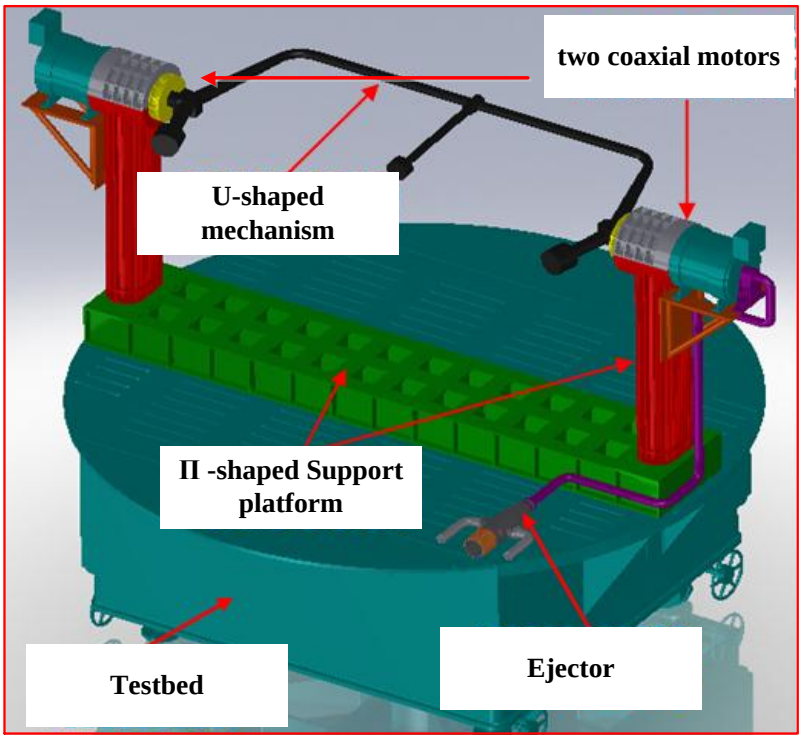

Figure 1- Schematic diagram of experimental support device of maneuvering inlet

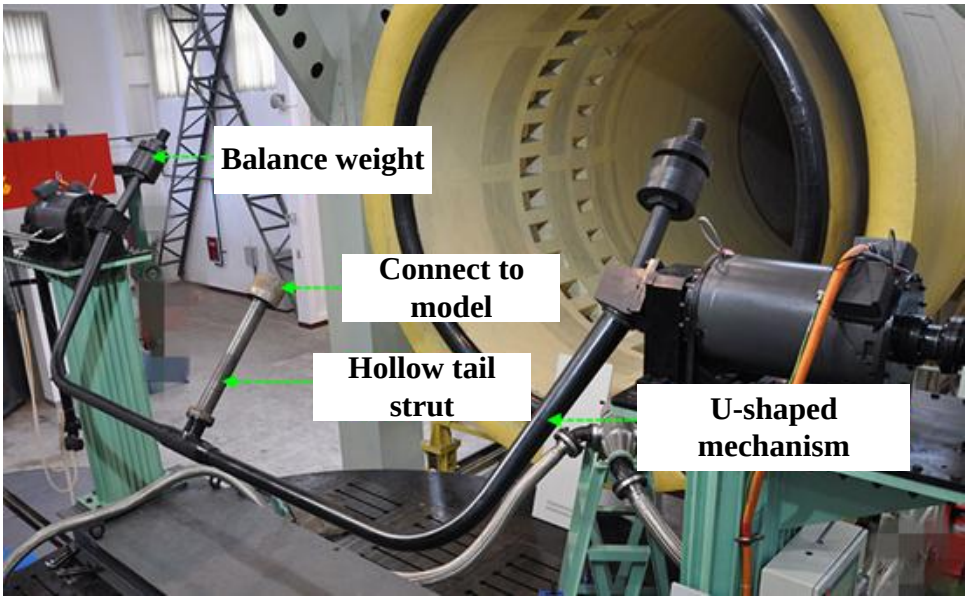

Figure 2- Photo of mechanical inlet experimental support device

2.3 Model and measurement system

The experimental model is a double belly inlet aircraft model. The length, width and height of model are 1.0m, 0.6m and 0.3m, respectively. And the weighs is about 18kg. The plugging degree of the model to the wind tunnel is about 0.9%. In the experiments, only the aerodynamic characteristics at AIP of the left inlet along the heading of the model were measured. The measuring section of the model is shown in Figure 3, in which 8 measuring rakes are contained, 5 pulsating pressure measuring points are set on each measuring rake, and 8 dynamic static pressure measuring points are set on the inner wall of the measuring section. In addition, the high-precision angular displacement potentiometer installed at one end of the torque motor rotation axis can measure

simultaneously the angle of attack during the model maneuvering process. The sampling frequency of pulsating pressure and angle of attack data is 20 kHz.

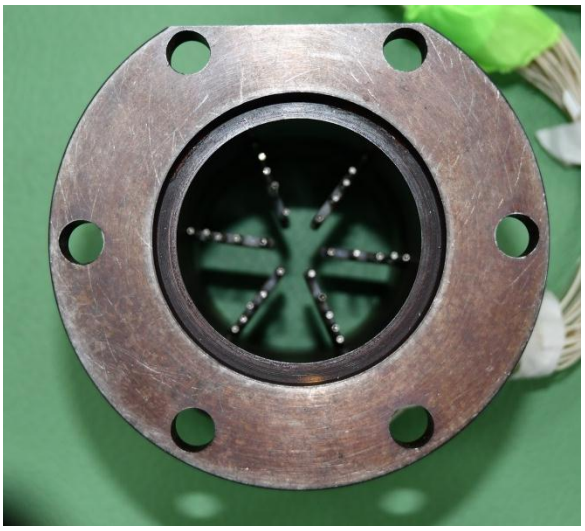

Figure 3- Photos of model measurement section

3. Experimental methods

3.1 Experimental procedure

In the steady-state experiment, the angle of attack and sideslip is fixed. The air flow in inlet is controlled by changing the state of opening or closing of the digital valves. The pressure data in measurement section would be collected after the flow field is stable. The performance parameters at AIP under different suction mass flow will be obtained. By changing the attitude angle of the model, the above work was repeated to obtain the inlet performance parameters at AIP for different attitude angles.

In the maneuvering inlet experiment, the mass flow in ejector was fixed. After the flow field in inlet was stabilized, the U-shaped support moved rapidly with a given angular speed. During the maneuvering process of the model, the PXI dynamic acquisition system would collect the data of pressure and angle of attack simultaneously. In the process of simulating sideslip maneuver, the model was rotated 90 degrees and installed on the U-shaped support, and the U-shaped support was used to drive the model motion with sideslip maneuver.

3.2 Calculation procedure

During the experiment, the total pulsating pressure values $\tilde{P}_{t\_ij}(t)$ and the static pulsating pressure values $\tilde{P}_{s\_j}(t)$ on the measurement section and the angle of attack values $\alpha(t)$ of model will be obtained, where *I* =1, 2... 5 is the number of measuring points on each rake, where j=1, 2... 8, is the serial number of rake. Since the pulsating pressure and angle of attack are collected synchronously and simultaneously, the total pulsating pressure value can be written as a function of angle of attack $\bar{P}_{ij}(\alpha)$, and the pulsating static pressure value can be express as $\bar{P}_{sj}(\alpha)$. The performance parameters in AIP can be calculated through $\bar{P}_{ij}(\alpha)$ and $\bar{P}_{sj}(\alpha)$.

The total pressure recovery coefficient of the inlet outlet section can be expressed as

$$\sigma_m(\alpha) = \bar{P}_{0m}(\alpha) / P_{0\infty} \qquad (1)$$

Where, $\bar{P}_{0m}(\alpha) = \sum_{i=j=1}^{i=I,j=J} \bar{P}_{ij}^2(\alpha) \cdot q(\pi_{ij}) \cdot \Delta A_{ij} \Big/ \sum_{i=j=1}^{i=I,j=J} \bar{P}_{ij}(\alpha) \cdot q(\pi_{ij}) \cdot \Delta A_{ij}$, $P_{0\infty}$ is the total pressure in the center of

experimental section of wind tunnel. I=5 is the number of total pressure measuring points on a single rake, and J=8 is the total number of rakes. ΔA_{ij} is the area corresponding to the single pressure measuring points. $q(\pi_{ij})$ is the flow function, which can be expressed as

$$q(\pi_{ij}) = \sqrt{14.9299 \cdot \pi_{ij}^{1.4286} \cdot (1 - \pi_{ij}^{0.2857})} \tag{2}$$

Where $\pi_{ij} = \bar{P}_s / \bar{P}_{ij}(\alpha)$, $\bar{P}_s = \frac{1}{J} \cdot \sum_{j=1}^{J} \bar{P}_{sj}(\alpha)$.

The flow coefficient $\varphi_m(\alpha)$ and mass flow G_m of AIP can be expressed as:

$$\phi_m(\alpha) = \sum_{i=j=1}^{i=I,j=J} \bar{P}_{ij}(\alpha) \cdot q(\pi_{m-ij}) \cdot \Delta A_{ij} \Big/ \bar{P}_{0\infty} \cdot A_{th} \tag{3}$$

$$G_m = [c \cdot \sum_{i=j=1}^{i=I,j=J} \bar{P}_{ij}(\alpha) \cdot q(\pi_{ij}) \cdot \Delta A_{ij}] \Big/ \sqrt{T_{0\infty}} \tag{4}$$

Where A_{th} is the throat area of the inlet, c=0.0404, and $T_{0\infty}$ is the total temperature in the experimental section of wind tunnel.

The steady-state circumferential distortion index can be calculated by the following procedure:

a. Calculating surface arithmetic mean total pressure recovery coefficient:

$$\bar{\sigma}_2 = \frac{1}{I \times J} \sum_{i=1}^{I} \sum_{j=1}^{J} \sigma_{ij} \tag{5}$$

Where $\sigma_{ij} = \bar{P}_{ij}(\alpha) / P_{0\infty}$. The average total pressure recovery coefficient of the J rake can be expressed as

$$\sigma_j = \frac{1}{I_1} \sum_{i=1}^{I_1} \sigma_{ij} \tag{6}$$

b. According to the circumferential position angle θ of each rake, connect σ_j with a straight line to obtain the continuous function $\sigma(\theta)$; looking for the number of low-pressure areas (the area of low-pressure is defined as the total pressure recovery coefficient less than $\bar{\sigma}_2$), and use linear interpolation to find the regional boundary θ_{k1} and θ_{k2}, where K is the number of low-pressure areas, as shown in Figure 4.

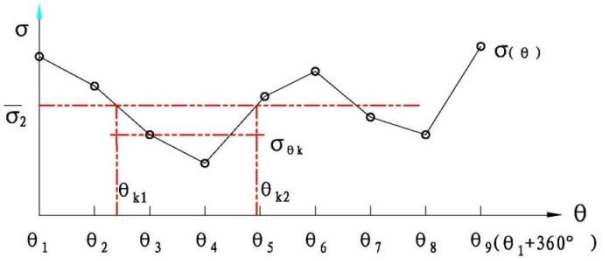

Figure 4- Schematic map for calculating the circumference distort index

c. Calculating the average total pressure recovery coefficient of each low pressure zone

$$\sigma_{\theta k} = \frac{1}{\theta_{k2} - \theta_{k1}} \int_{\theta_{k1}}^{\theta_{k2}} \sigma(\theta) d\theta \tag{7}$$

d. Calculating the circumferential distortion index of each low pressure zone

$$\Delta\sigma'_{\theta k} = [(\bar{\sigma}_2 - \sigma_{\theta k})/\bar{\sigma}_2] \times 100\% \quad (8)$$

e. For the occurrence of multiple low-pressure areas, do the following processing:

If $\Delta\theta_k = \theta_{k2} - \theta_{k1} \geq 60°$, then $\Delta\sigma_{\theta k} = \Delta\sigma'_{\theta k}$. If $\Delta\theta_k < 60°$ then $\Delta\sigma_{\theta k} = (\Delta\theta_k / 60°) \cdot \Delta\sigma'_{\theta k}$.

Finally, the steady-state circumferential distortion index is obtained by $\Delta\sigma_\theta(\alpha) = \max\{\Delta\sigma_{\theta k}\}$.

The turbulence is calculated from the pulsation pressure at the location of the 90% radius. The pulsation pressure value $\tilde{P}_{dj}(\alpha)$ consists of a series of pressure value $P_{dj\_n}(\alpha)$, where n=1, 2... N, N is 100; The turbulivity of a single pulsating pressure measurement point can be expressed as:

$$Tu_j(\alpha) = \frac{\sqrt{\frac{1}{N}\sum_{n=1}^{N}(P_{dj\_n}(\alpha) - \bar{P}_{dj}(\alpha))^2}}{\bar{P}_{dj}(\alpha)} \quad (9)$$

Where $\bar{P}_{dj}(\alpha) = \frac{1}{N}\sum_{n=1}^{N}\tilde{P}_{dj\_n}(\alpha)$ is the mean value of pulsating pressure. The mean turbulence of AIP is

$$Tu_m(\alpha) = \frac{1}{J}\sum_{j=1}^{J} Tu_j(\alpha) \quad (10)$$

The comprehensive distortion index is the sum of turbulence and circumferential distortion index.

$$W_m = Tu_m + \Delta\bar{\sigma}_{0m} \quad (11)$$

For the maneuvering inlet experiment, the variation curve of aerodynamic characteristic parameters at AIP with angle of attack can be obtained at a certain suction flow and at a certain angular velocity of model. For the steady-state inlet experiment, the angle of attack measured by the Angle of attack sensor only fluctuates slightly because the Angle of attack does not change, so the aerodynamic characteristic parameters can be averaged directly.

4. Experimental results

In order to verify the reliability of the experimental system, a repeatable test was carried out. Figure 5 shows the repeatable test results of the performance parameters at AIP with different Flow coefficient ϕ when V=60m/s, α=0°, β=0°, and Table 1 shows the difference of aerodynamic characteristic parameters at AIP of inlet/engine working matching points two repeatability experiments. The results in Table 1 show that the repeatability deviation of the flow coefficient ϕ, total pressure recovery coefficient σ, turbulence Tu, steady-state circumferential distortion $\Delta\sigma_\theta$ and comprehensive distortion index at matching point value for the two independent tests in the same state is 0.001, 0.000, 0.0001, 0.0003 and 0.0004, respectively. Figure 6 shows the repeatability test results of three independent tests of the model under the pitching maneuver condition of ω_α=240°/s, V=60m/s. It can be seen from the figure that the repeatability of the curves of the three repeatability tests is good. The repeatability results of steady-state and maneuvering inlet experiments show that the experimental system has good stability and reliability.

Table 1 The difference of performance parameters for two repeatability experiments

Parameters	ϕ	σ	$\Delta\sigma_\theta$	Tu	W
Difference	-0.001	0.000	-0.0003	-0.0001	-0.0004

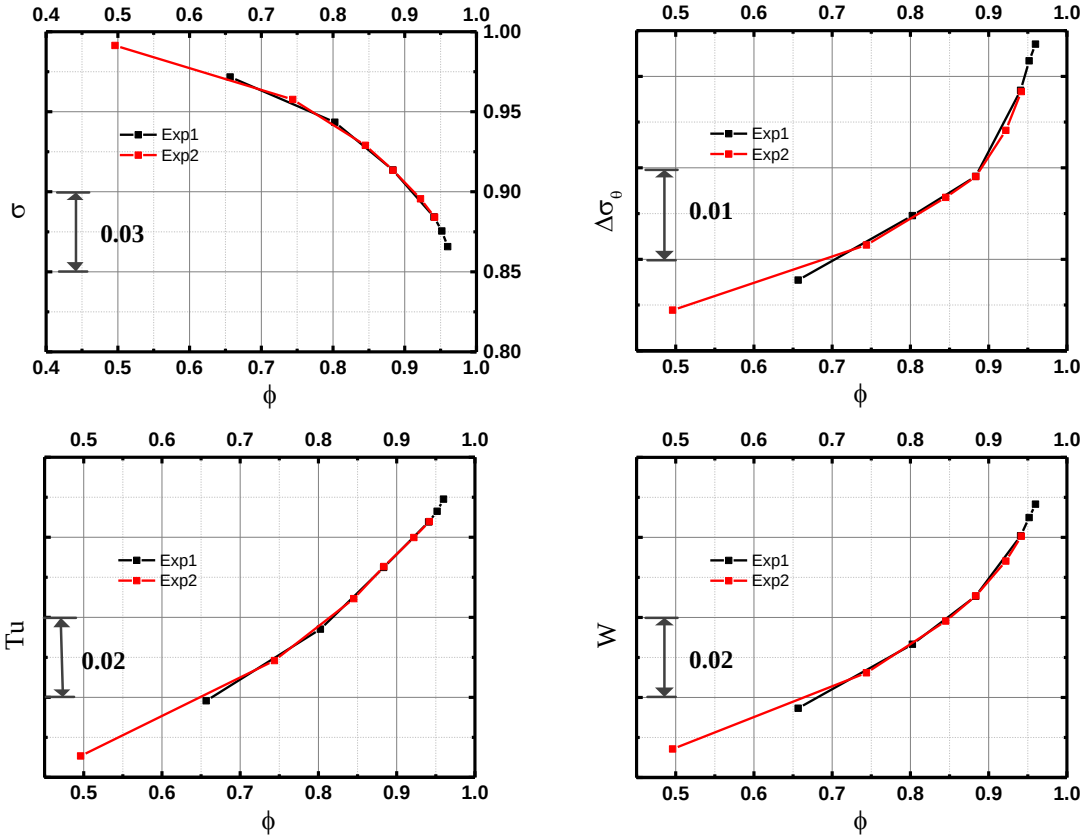

Figure 5- Repeatability experimental results of steady inlet

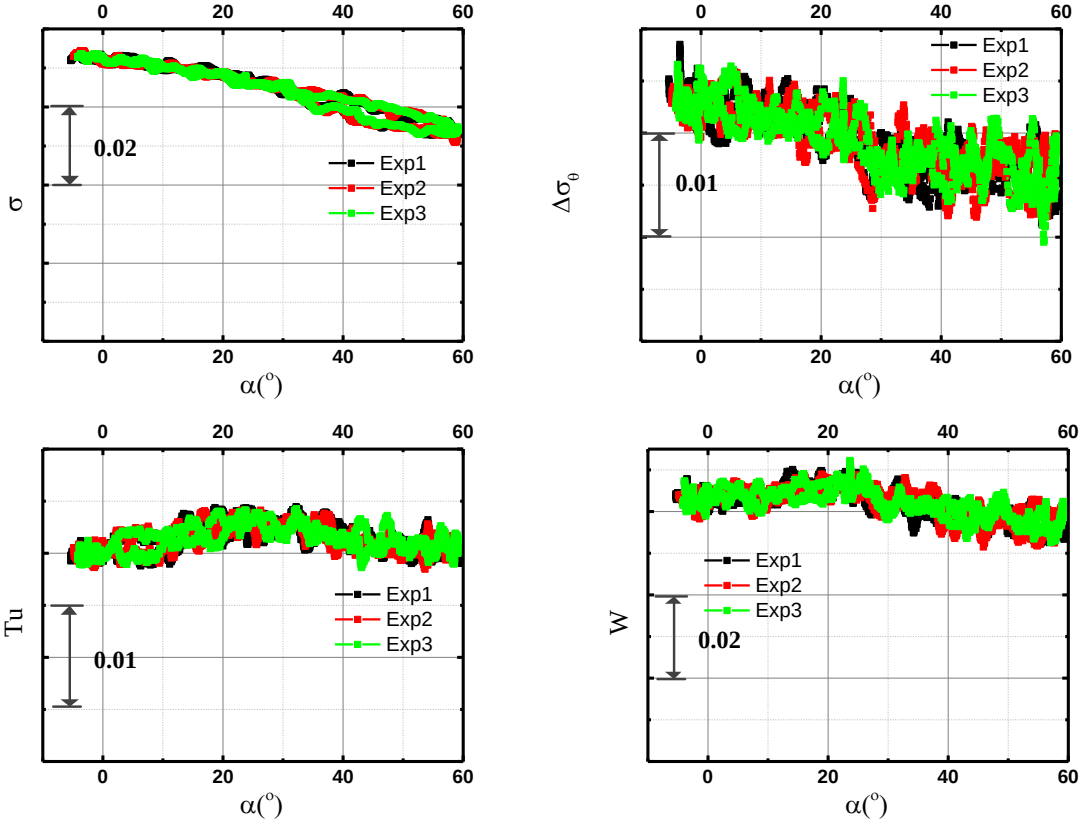

Figure 6- Repeatability experimental results of maneuvering inlet

Figure 7 compares the inlet experimental results of steady-state with the experimental results of pitching maneuver process at the condition of ω_α=240°/s, V=60m/s and β=0°. It results show that the total pressure recovery coefficient in steady state is just slightly different from that in pitching maneuver process. The total pressure recovery coefficient in the steady state is roughly between the upward and downward pitching maneuver of the model. In addition, the maneuvering experiment results show that the total pressure recovery coefficient curves of the model's upward and downward pitching maneuver do not strictly coincide, and the total pressure recovery coefficient of downward pitching maneuver is significantly greater than that of upward pitching maneuver when the angle of attack is between -80°~10° and 30°~100°. The comprehensive distortion index of steady-state experiments and pitching maneuver experiments have the same trend varying the angle of attack. In most angle range, the comprehensive distortion index of pull-up maneuver is slightly larger than that of steady state. For example, at α=75°, the composite distortion index at the state of model pull-up with angular speed ω_α=240°/s is 0.015 larger than the corresponding value of the steady-state.

Figure 8 compares the experimental results of steady-state with the sideslip maneuvers at ω_β=240°/s , V=60m/s and α=0°. The experimental results show that the total pressure recovery coefficient of sideslip maneuvers experiment has significantly difference with steady-state experiment at the angle of sideslip β=-40°~40°. The total pressure recovery coefficient of steady-state experiment at β=10° is 0.01 larger than that of sideslip maneuvering. In most sideslip angle range, the total pressure recovery coefficient of left-turn maneuver is smaller than right-turn maneuver. The comprehensive distortion index of steady-state experiments and the sideslip maneuver have the same trend varying the sideslip angle. In most sideslip angle range, the comprehensive distortion index of sideslip maneuver is slightly larger than that of steady-state test. For example, the comprehensive distortion index of turn-left maneuver experiments at condition of ω_β=240°/s, α=0° is 0.003 larger than the value of the steady-state test.

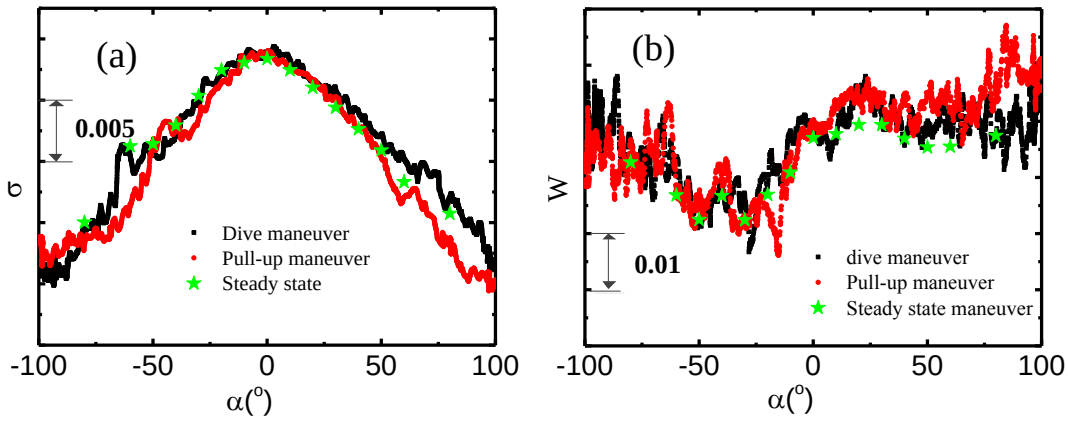

Figure 7 – The curves of total pressure recovery coefficient (a) and comprehensive distortion index (b) for belly inlet under the steady state and the pitching maneuver state of ωα= 240°/s, V=60m/s.

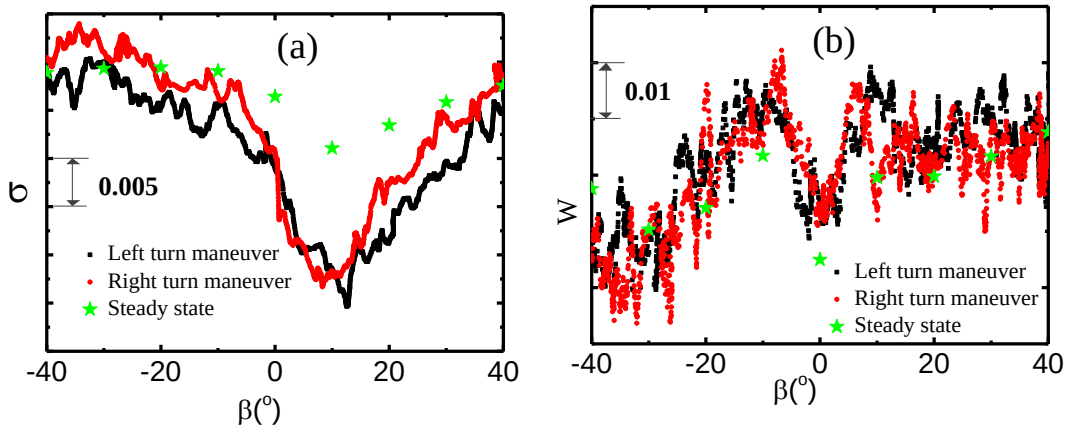

Figure 8 – The curves of total pressure recovery coefficient (a) and comprehensive distortion index (b) for belly inlet under the steady state and the sideslip maneuver state of ω_β= 240°/s, V=60m/s.

Conclusion

In the Φ-3.2m wind tunnel of China Aerodynamics Research and Development Center, steady-state and maneuvering inlet experiments were carried out for an aircraft model with belly inlet, and the influence of maneuvering process on the performance of belly inlet was research. The research results can be concluded as follows:

1. For the aircraft with belly inlet, the pitching maneuver has little influence on the total pressure recovery coefficient and comprehensive distortion index at the experiment condition of wind speed V=60m/s, β=0° and angular speed of ω_α=240°/s. The sideslip maneuver has great influence on the total pressure recovery coefficient and little effect on the comprehensive distortion index at AIP at the experiment condition of V=60m/s, α=0°and angular speed of ω_β=240°/s.
2. The aerodynamic characteristics at AIP for steady state and maneuver state of aircraft with belly inlet exists certain differences. The experimental result of steady state can not accurately describe the aerodynamic characteristics of aircraft under the maneuver condition. Especially, for the highly mobility fighter with abdominal inlet, the effect of maneuver process on the aerodynamic characteristics at AIP should be evaluated.

References

[1] McCallum B. F-16 Inlet Stability Investigation[R].AIAA 89-2465,1989.

[2] Norby W P, Hleffele B A and Burley R R. Isolated Testing of Highly Maneuverable Inlet Concepts[R].NASA Contractor Report- 179544, 1986.

[3] Kevin R W, Andrew J Y, John G W, et al. Inlet Distortion for an F/A-18A Aircraft During Steady Aerodynamic Conditions up to 60° Angle of Attack[R]. NASA Technical Memorandum 104329, 1997.

[4] Andrew J Y, William G S, John G W, et al. F/A-18A Inlet Flow Characteristics During Maneuvers with Rapidly Changing Angle of Attack [R]. NASA Technical Memorandum 104327, 1997.

[5] Steenken W G and Williams J G, Yuhas A J, et al. Factors Affecting Inlet-Engine Compatibility During Aircraft Departures at High Angle of Attact for an F/A-18A Aircraft [R].NASA/TM- 206572,1999.

[6] William G S, John G W, Andrew J Y, et al. An Inlet Distortion Assessment During Aircraft Departures at High Angle of Attack for an F/A-18A Aircraft[R]. NASA Technical Memorandum 104328, 1997.

Copyright Statement